THE ASTROPHYSICAL JOURNAL, 209:858–867, 1976 November 1

Hα POLARIZATION AND LINE PROFILES IN WHITE DWARFS WITH STRONG MAGNETIC FIELDS

ERMANNO F. BORRA
Département de Physique, Université Laval, Quebec, Canada
Received 1975 December 11; revised 1976 March 12

ABSTRACT

Hα circular polarization and intensity profiles in white dwarfs with strong magnetic fields are computed for dipole and dipole-like configurations of the magnetic field. The polar fields vary from 4×10^7 to 10^8 gauss. The profiles are severely distorted by the strong nonhomogeneous fields. They are strongly dependent on field strength and magnetic geometry. An interesting and potentially very useful feature of the profiles is the appearance of sharp σ^+ (red) components. The wavelength location of those components is fairly insensitive to field strength: either they are not there or they are at the correct wavelength. This makes them useful in identifying Hα in magnetic white dwarfs. The intensity and polarization spectra of known magnetic white dwarfs are examined in the light of the models.

Subject headings: line profiles — polarization — stars: magnetic — stars: white dwarfs — Zeeman effect

I. INTRODUCTION

Until quite recently, all the known magnetic white dwarfs were found because of their continuum polarization. All of those objects had peculiar or featureless spectra. Searches for magnetic fields in DA white dwarfs were unfruitful (Angel and Landstreet 1970; Preston 1970; Trimble and Greenstein 1972). This lack of magnetic DA's could be due to the fact that observers concentrated mostly on peculiar objects rather than DA's. This can readily be ascertained by perusing the literature and from the list of null measurements in Angel, Landstreet, and Borra (1976). Also, the searches were conducted mostly in broad-band continuum observations; fields of less than a million gauss might have been missed. The more sensitive method of narrow-band observations in the wings of a spectral line was used for only a few stars. As far as the use of the quadratic Zeeman effect is concerned, it is not very sensitive; the interpretation of the observational data is not easy (Borra 1973), and magnetic fields might have been missed.

In view of the late discovery of hydrogen lines in at least two magnetic white dwarfs (Liebert, Angel, and Landstreet 1975; Angel *et al.* 1974), it is legitimate to suspect that other magnetic DA's exist and will be found. However, because the shape of the Balmer lines can be greatly affected by the magnetic field, recognizing the hydrogen spectrum in a magnetic white dwarf might be quite difficult. The spectrum of hydrogen in strong magnetic fields (Garstang and Kemic 1974; Lamb and Sutherland 1973; O'Connell 1974) is complex as the *l*-degeneracy is removed. For sufficiently strong fields the Balmer spectrum is spread over several thousand angstroms, giving very shallow and wide features—too shallow to be detected with present techniques. If some relatively sharp features are present, they might be at wavelengths quite different from the usual Balmer rest wavelengths. Thus, especially for nonhomogeneous geometries of the magnetic field and very strong fields, a DA could be mistaken for a peculiar or featureless object. Indeed, GD 90 was at first thought to be a peculiar object and G99–47 a featureless one. Searching for continuum polarization in a DA white dwarf easily recognizable as such is thus an invitation to failure, as the simple fact that the Balmer lines are recognizable implies that the field is not very strong.

II. INFLUENCE OF THE MAGNETIC FIELD ON HYDROGEN LINES

Borra (1973) has computed Balmer line profiles for dipole and dipole-like fields of about 10^6 gauss. The lines are asymmetrical, the red wing being steeper than the blue one. The effect is not large and might not be recognized visually. Hδ and Hγ profiles by Borra (1973) and Hγ and helium line profiles by Kemic (1974*a*) for fields of the order of 5×10^6 gauss show dramatic effects on the profiles.

The lines are greatly broadened and highly asymmetrical, resembling the profiles observed in GD 90. For fields greater than 10^7 gauss, the high Balmer lines will be spread over several hundred angstroms, blended with each other and very shallow. It will be difficult, if not impossible, to recognize and interpret the blue spectrum of such a DA. The line profiles are exceedingly sensitive to the strength and the geometry of the magnetic field.

As the quadratic Zeeman effect is (in the first order) proportional to the fourth power of the principal quantum number *n* and the linear Zeeman effect is easier to recognize and interpret, and is proportional to the square of the wavelength of the spectral line, it

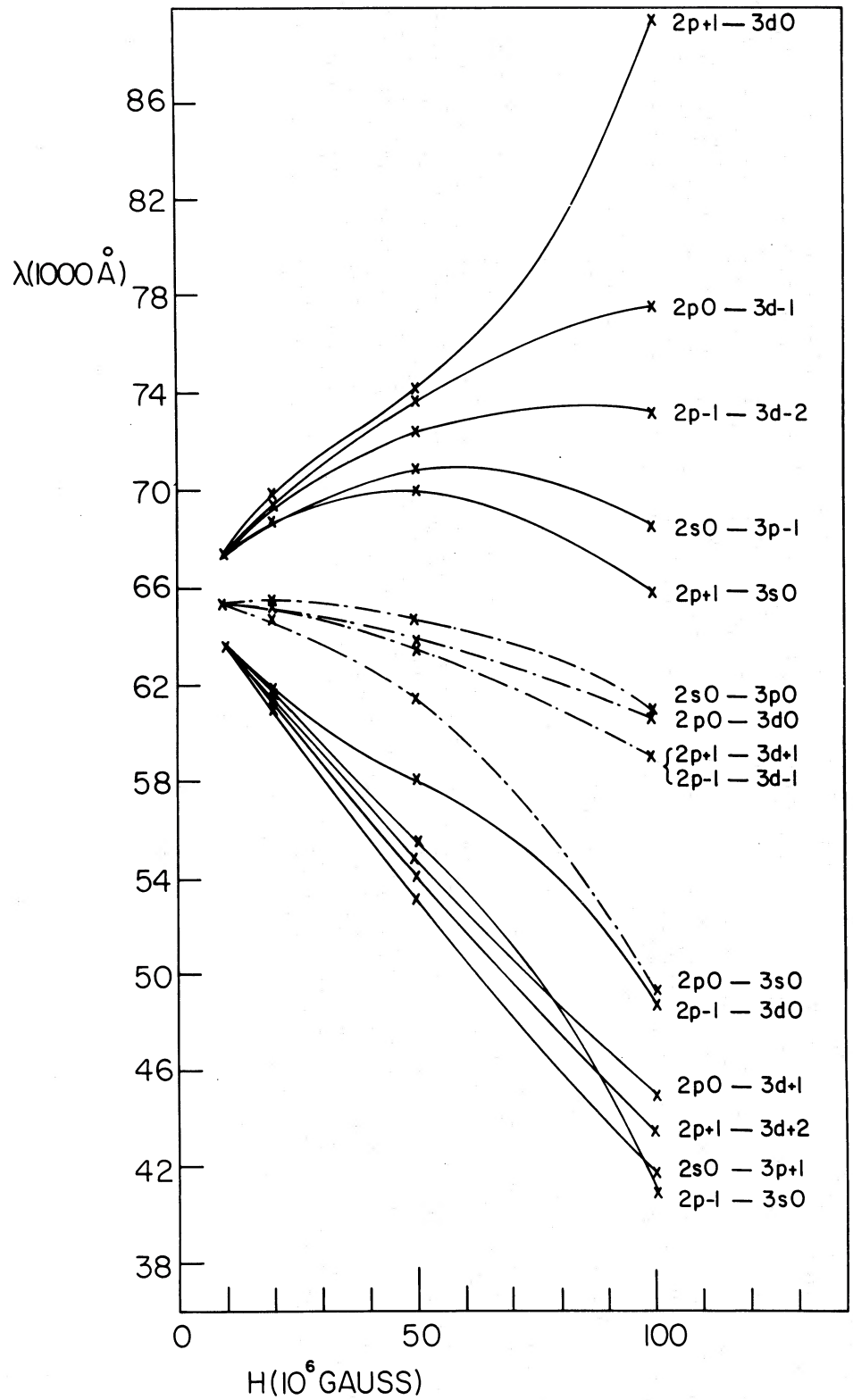

FIG. 1.—Structure of the σ^+, σ^-, and π components (*broken line*) of Hα in very strong magnetic fields. The components are identified by their transition.

appears preferable to use Hα to search for and interpret magnetic DA's. Figure 1 shows the wavelength location of the various components of Hα as a function of the magnetic field strength. The figure has been drawn using Kemic's tabulations (1974*b*). Kemic's computed values are indicated as crosses. The curves through his points are least-squares-fitted cubics. The theory and computations have been described by Garstang and Kemic (1974). The advantages in using Hα can immediately be seen from Figure 1. The linear Zeeman effect dominates in most of the range covered. For fields as high as a few times 10^7 gauss the spread within the π and σ components is small and the Zeeman splitting of the line can still be fairly well represented by a triplet. Figure 1 also makes apparent another characteristic of Hα: even for fields as high as 10^8 gauss the linear effect still dominates over the quadratic in that there is no overlap among the π and σ components. In particular, the σ^+ components are still longward of the rest wavelength of Hα.

Liebert, Angel, and Landstreet (1975) have also computed Hα profiles they compare with the quadratically shifted Hα in G99–47.

III. THEORETICAL LINE PROFILES

Although Figure 1 shows that Hα has (for sufficiently low fields) mostly a relatively simple (but broadened) triplet structure, the line profiles resulting from a nontrivial geometry of the magnetic field (such as a constant field) can be more difficult to recognize. This is because the observed profile is the sum of the profiles formed in parts of the visible disk having different values of field strength and orientation of the field lines. As examples of the variety of profiles that one might encounter, I have computed Hα profiles for a number of magnetic geometries and magnetic field strengths.

The computer program used is the same as that described by Borra (1973). It subdivides the visible disk of a star with a given field geometry in about 600 slices and computes, for each slice, the line and polarization profiles using Unno's solutions for the equations of transfer for a spectral line formed in the presence of a magnetic field, within the Milne-Eddington approximation. Finally, the program synthesizes the observed line and polarization profiles. In Borra (1973) the Balmer lines were treated as triplets, an approximation valid for sufficiently low magnetic fields. At the higher magnetic fields we will consider, this approximation is no longer valid and we must treat in full the more complicated Zeeman structure of Hα: 10 σ components and four π-components. It is interesting to notice that even though the triplet approximation used to compute profiles of Hδ and Hγ is no longer valid at fields of 5×10^6 gauss, the profiles in Borra (1973) show the same general characteristics as the profiles in Kemic (1974*a*) who uses the more complex structure. This illustrates well the fact that the most important factor in this type of calculation is the degree of nonhomogeneity of the magnetic field and the field strength.

The wavelength location of each component as a function of field strength was found by a polynomial fit (a cubic) to Kemic's (1974*b*) tabulation of wavelengths and strengths of hydrogen transitions in large magnetic fields. The polynomial fits give the lines in Figure 1. The uncertainties in wavelength locations due to the fit are difficult to evaluate but, hopefully, should not be at worse greater than a few tens of angstroms. More extensive tabulations are desirable in order to improve the fit. These uncertainties are not a serious problem because, as we will see later, the smearing of the profiles due to the geometry of the magnetic field dominates the profiles.

The wavelength dependence of the absorption coefficient for each component is taken to be of the form (Aller 1963)

$$K(\Delta\lambda) = C_n E_0^{3/2}[1 + R(N, T)(\Delta\lambda)^{1/2}]/\Delta\lambda^{5/2} . \quad (1)$$

At the strong fields we consider, the *l*-degeneracy is removed and this formula (which assumes *l*-degeneracy) is no longer rigorously valid. However, the nonuniformity of the magnetic field, through Zeeman broadening, is by far the dominant effect on the lines. The errors introduced by the use of equation (1) are totally negligible. Any formula reproducing the approximate width and depth of Hα in zero field is quite adequate. The parameters of the Milne-Eddington approximation were chosen so as to reproduce, for zero field, the width and depth of Hα in a "typical" strong-lined DA. Thus, when comparing the profiles with a DA candidate we should give allowance for differing line strengths.

IV. THE COMPUTATIONS

Figures 2–7 show the Hα profiles for centered and decentered dipole geometries. The profiles are identified by the polar magnetic field strength and the inclination of the axes of the symmetry of the dipole with respect to the line of sight. These figures illustrate the changes occurring when we vary the polar strength of the field and the viewing angle.

For the strongest fields (H_p = 80 million and 100 million gauss) Hα is spread over a few thousand angstroms. The σ^- component is far too shallow and spread-out by the nonhomogeneity of the magnetic field to be detected with today's techniques. The π-component is also quite shallow but should be detectable. The most important and interesting feature of these figures is the appearance of relatively sharp and deep features in the σ^+ (red) component. These features arise because some of the σ^+ components resist the spreading-out effect of the magnetic field. To understand this, consider figure 1. We can see that for some intervals of field strength the wavelength location of some of the components varies only very slowly with the field. This is the case for the $2P_{+1}$–$3S_0$ component for $3 \times 10^7 < H < 6 \times 10^7$ gauss, the $2S_0$–$3P_{-1}$ component for $5 \times 10^7 < H < 7 \times 10^7$ gauss, and $2P_{-1}$–$3D_{-2}$ component for $6 \times 10^7 < H < 10^8$ gauss. This occurs near the point at which,

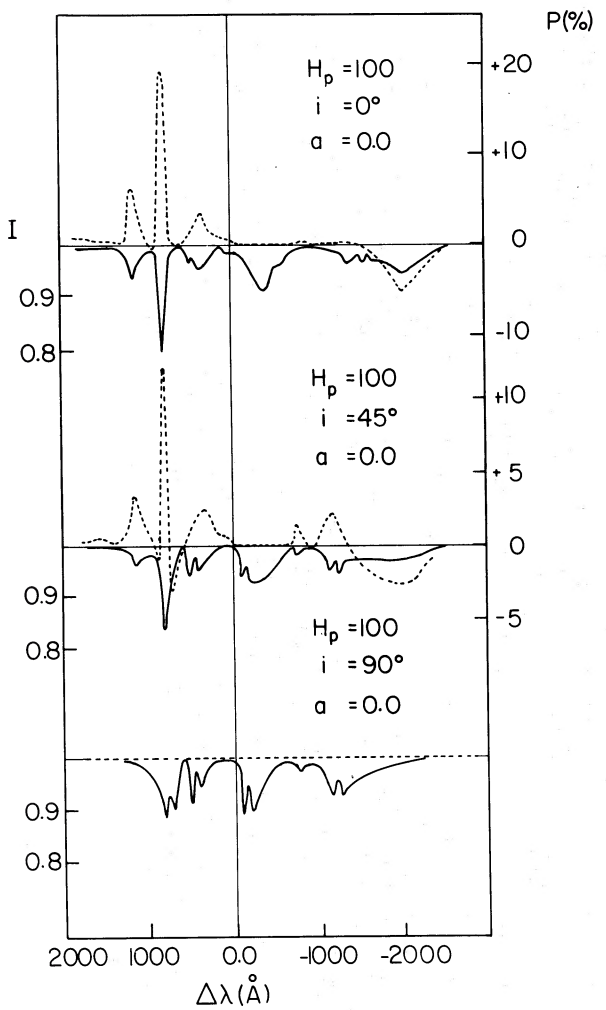

FIG. 2.—Intensity (*solid line*) and percentage circular polarization (*broken line*) structure in Hα for a dipolar field ($a = 0.0$). The polar field H_p is 100 million gauss. The three pairs of profiles correspond to different inclinations of the magnetic axes on the line of sight ($i = 0°0$, 45°, 90°).

for every component, the violet quadratic shift becomes more important than the red linear Zeeman shift. This provides us with relatively sharp and deep intensity and polarization components potentially extremely useful as clues to identifying Hα and as measures of the magnetic field strength and structure. It is especially fortunate that as soon as a particular component is no longer sharp, a new one becomes usable. For fields greater than 10^8 gauss we can expect that the $2P_0$–$3D_{-1}$ component and the $2P_{+1}$–$3D_0$ component will give sharp features in certain field ranges. At this stage, let us sound a note of caution: Kemic's tables have big gaps in field strength; the values in between are given by polynomial fits. The effect mentioned is valid for those polynomial fits. Even though the shapes of the polynomial appear plausible, the exact shape of the curves should be determined.

Although the line profiles for strong fields (and especially for lower equivalent widths) might not be detectable with present techniques, the polarization structure introduced by Hα will be detectable and can contribute much structure to any continuum polarization.

A remarkable feature of Figures 2 and 3 is that the number and location of the sharp σ^+ components depends on the strength of the magnetic field and the inclination of the dipole. The changes appearing in the $H_p = 80$ model, when changing the angle of inclination are especially striking. We see at the inclination of 45° a reversal of the sign of polarization in both the σ^+ and the σ^- components and the apparition of a different σ^+ with opposite polarity. This can easily be understood; when viewing the dipole at 45°, we see strong regions with positive longitudinal field, giving a large shift with positive polarization and weaker regions of negative field giving negative polarization with a smaller wavelength shift; thus a positive polarization sign appears to the red of the negative polarized σ^- components. The sharp new component at an angle of 45° appears because the

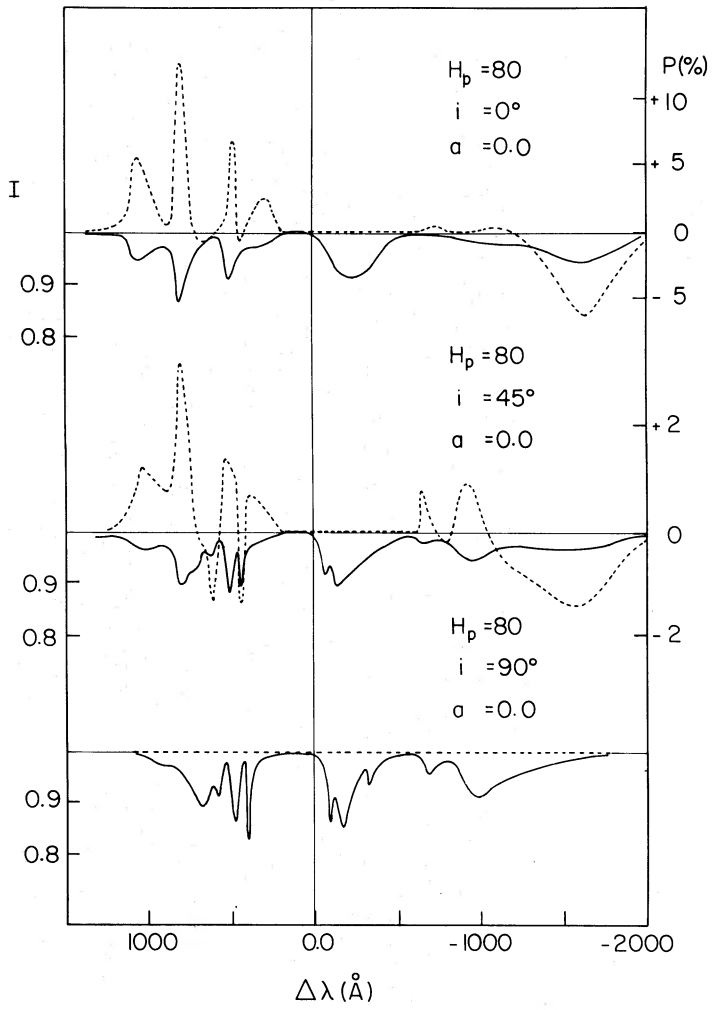

FIG. 3.—Intensity (*solid line*) and percentage circular polarization (*broken line*) structure in Hα for a dipolar field ($a = 0.0$). The polar field H_p is 80 million gauss. The three pairs of profiles correspond to different inclinations of the magnetic axes on the line of sight ($i = 0°.0, 45°, 90°$).

regions of negative longitudinal field are in the field range in which the position of the $2P_{+1}$–$3S_0$ component is almost independent of field strength. If such a star exists in nature and rotates, the spectral changes will be considerable. Notice also that in Figure 2*a* the σ^+ components give the amusing and misleading impression of a Zeeman triplet centered at about 7400 Å.

The cases $H_p = 80$, $a = 0.1$ and 0.4 (Figs. 4 and 5) illustrate cases of greater inhomogeneity of the magnetic field; a is a decentering parameter expressed in units of the stellar radius and indicating the amount by which the center of symmetry of the dipole is displaced from the center of the star (Landstreet 1970). For these models we display the circular polarization profiles as well. For the model with $a = 0.1$ (Fig. 4), much the same things can be said as for the model with $a = 0.0$. The sign reversal of the circular polarization within the σ components occurs even when the dipole is seen pole-on, as regions of opposite magnetic polarity are visible over the disk. Sharp components are still present. The detailed shapes of both polarization and line profiles are different from the centered-dipole case, as we would have expected.

For $a = 0.4$, viewing the strongest pole on the surface of the star along the line of sight (angle is 0.0), we can easily recognize a typical S-shaped polarization signal which originates from the regions of low field. The line profile does not look the least like a Zeeman triplet. The regions of higher field give extended wings to the line profile, too weak to be detected. The polarization contributed by these regions is, however, sizable, and should be easily detected. Viewing the weakest pole (inclination of 180°), the line is clearly a Zeeman triplet as the surface field is small.

For centered dipoles at lower fields ($H_p = 60$ and 40, Figs. 6 and 7) Hα appears more and more as a triplet with deeper and therefore more easily detectable components. For $H_p = 60$, Hα is still split into several components both in the line and

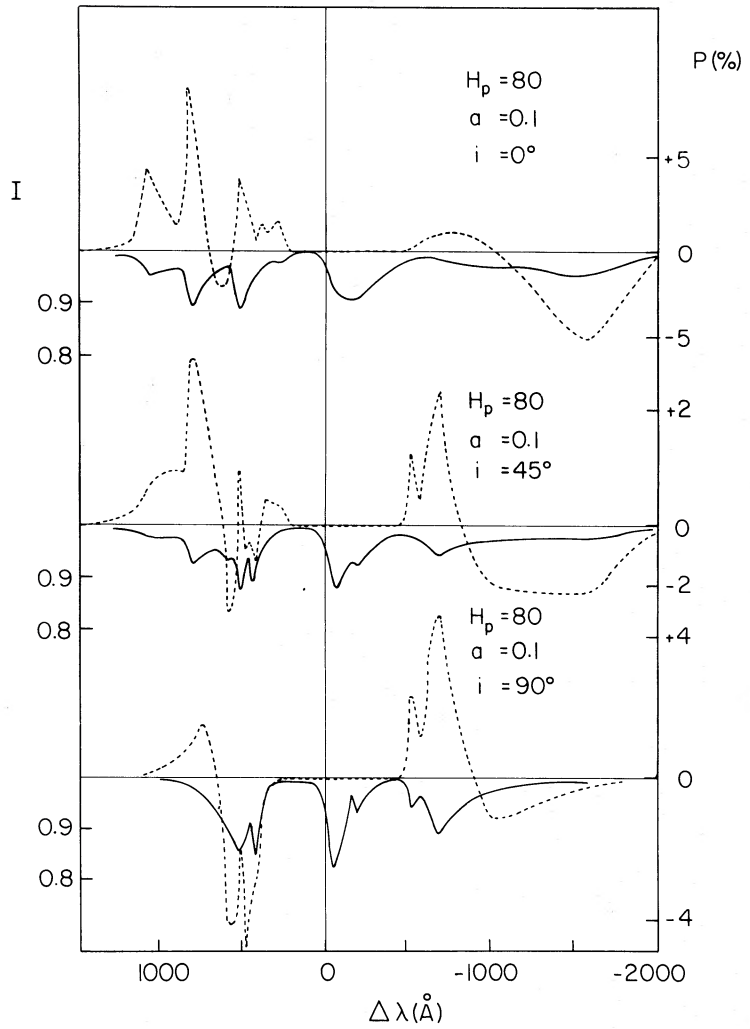

FIG. 4.—Intensity (*solid line*) and percentage circular polarization (*broken line*) structure in Hα for a displaced dipole field with decentering parameter (a = 0.1). The three pairs of profiles correspond to different inclinations of the magnetic axes on the line of sight (i = 0°.0, 45°, 90°).

polarization profiles. At even lower fields (H_p = 40) the structure all but disappears and we are left with asymmetrical Zeeman triplets.

V. COMMENTS ABOUT KNOWN MAGNETIC WHITE DWARFS

Two magnetic white dwarfs are now known to have hydrogen lines. The white dwarf GD 90 was discovered to be magnetic purely on the basis of its Zeeman-split hydrogen lines (Angel *et al.* 1974) and has a field of 5 million guass. The continuum polarized white dwarf G99–47, previously thought to be featureless, shows a weak Hα and a field of 20 million gauss (Liebert, Angel, and Landstreet 1975). Recently, Wickramasinghe and Bessell (1976) found that BPM 25114 has features that could be due to quadratically shifted Balmer lines in a field of about 10^7 gauss; however, this still awaits confirmation from polarization measurements. In the discussion below, we will not consider those stars, as they have already been discussed in the above references. We will instead examine the other known continuum polarized stars. We will not make here great efforts to model those features but we will rather make some comments based on what we can learn from the present models.

a) GD 229

Multichannel intensity scans have been published by Greenstein, Schmidt, and Searle (1974) and Greenstein (1974). A circular polarization multichannel scan has been published by Landstreet and Angel (1974). The feature at ~4170 Å cannot be identified with the σ^- component of Hα; because of its sharpness it would imply a totally homogeneous field of about 10^8 gauss, and still be much too sharp. One runs into similar problems with the feature at ~5240 Å. A more interesting feature is the one at ~7100 Å. As we can

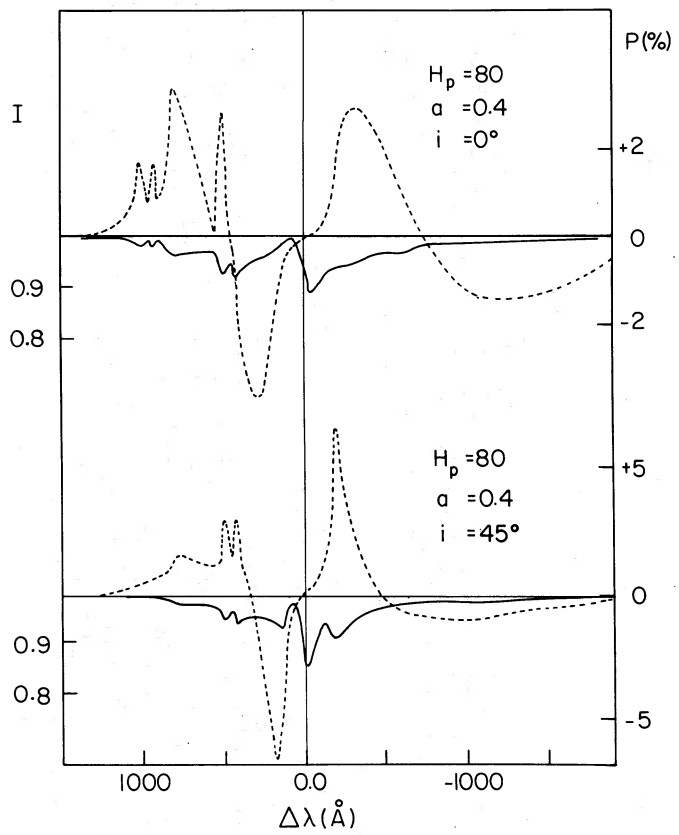

FIG. 5.—Intensity (*solid line*) and percentage circular polarization (*broken line*) structure in Hα for a displaced dipole field with decentering parameter ($a = 0.4$). The two pairs of profiles correspond to different inclinations of the magnetic axes on the line of sight ($i = 0°, 45°$).

see from Figures 2–6, there is always a grouping of components at about this wavelength. This is caused by a blend of the $2P_{+1}$–$3S_0$, $2S_0$–$3P_{-1}$, and $2P_{-1}$–$3D_{-2}$ components, mixed with different relative strengths depending on the geometry and field strength. Let us assume that we have correctly identified this feature as being due to Hα. This implies that we have fields between ~4 and 8×10^7 gauss over a significant portion of the visible disk. The σ^- components would be too broadened by the nonhomogeneous field to be visible, but the π-components should be detectable. Figure 1 of Greenstein (1974) shows a small dip at $1/\lambda < 1.6$ ($\lambda > 6250$ Å), although one might question the reality of the dip. A tentative identification of Hα in GD 229 hinges on the reality of this dip and its identification as the π-components. The scan of Greenstein, Schmidt, and Searle (1974) also shows a small dip at this wavelength whose reality one might also question, but which might add to our confidence. Among the theoretical models presented in Figures 2 to 7, the model with $H_p = 80$, $a = 0.1$, $i = 45°$ is probably the one that would match more closely the spectrum of GD 229 for $\lambda > 6500$ Å.

The published polarization scans show that there probably is some structure superimposed on the continuum polarization; however it is also clear that the contribution of this polarization is much less than the one we see in Figure 4. This might indicate that the geometry is different in details (although having about the same degree of inhomogeneity), that Hα is weaker in GD 229, or that Hα is not responsible for the features in question.

b) Grw +70°8247

Greenstein, Schmidt, and Searle (1974) find that this star has a spectrum resembling somewhat the one of GD 229. In particular, we can see the same feature at ~7100 Å and we we could have much the same discussion as for GD 229. However, now we do not see a convincing evidence of the π-components. There might be a small dip at ~6300 Å, although we might doubt seriously of its reality. In any event the π-feature should not be so much weaker than the σ^+ feature; this is contrary to the characteristics of all the models computed. The linear polarization scan published by Landstreet and Angel (1975) does not show a polarization step consistent with the presence of the π-components. The presence of Hα in Grw +70°8247 is even less convincing than it is in GD 229. The feature at ~7100 Å is more likely to be caused by some unknown absorber, possibly a molecular band. Considering that the same feature is present in GD 229, we might infer that it is caused by the same absorber in this star as well.

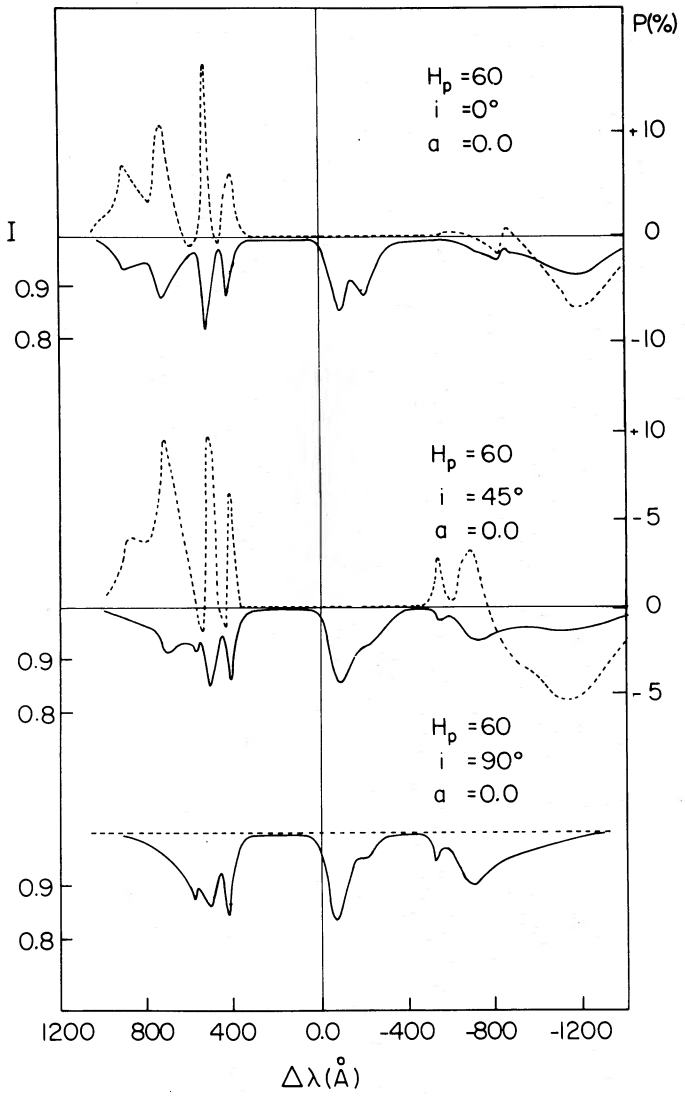

FIG. 6.—Intensity (*solid line*) and percentage circular polarization (*broken line*) structure in Hα for a dipolar field ($a = 0.0$). The polar field Hα is 60 million gauss. The three pairs of profiles correspond to different inclinations of the magnetic axes on the line of sight ($i = 0°.0, 45°, 90°$).

c) G240–72

An intensity scan is given by Greenstein (1974). The spectrum is rather peculiar in that it is continuous with a single strong and broad feature at least 2500 Å wide and with an equivalent width of about 240 Å. Greenstein speculates that it is caused by a quadratically shifted Hα blending with other Balmer lines. A first difficulty with this interpretation is (as recognized by Greenstein) that it is difficult to obtain such a strong Balmer line at the low temperature of G240–72 (~6000 K). Another problem is that, as mentioned earlier, Hα is not shifted to the blue as a single feature but has, for fields of less than 100 millions gauss, all of its σ^+ components longward of 6563 Å. It cannot, as a whole, give the feature in question. We can attempt to place the continuum differently. Judging from the published scan, we could see a continuation of the feature to about 7500 Å. Hα would now be spread over about 3000 Å! The equivalent width is now even greater and harder to believe. Even neglecting this fact, the author tried very hard to find a magnetic geometry (even including rotational Doppler broadening) to account for the feature but could not manage to reproduce the fact that the σ^- component would have to be deeper than the π and the σ^+ components. Again, we must conlude that we do not see evidence of Hα.

d) G99–37

A scan by Oke and Shipman (1971) does not show any red feature. Similarly a polarization scan by Angel and Landstreet (1974) does not show any feature that

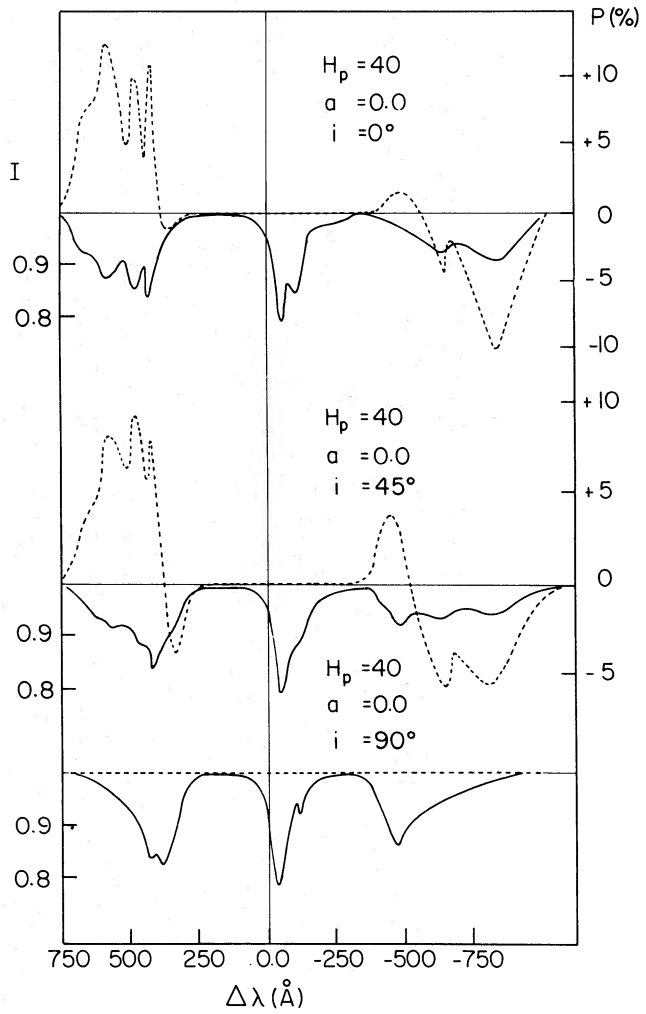

FIG. 7.—Intensity (*solid line*) and percentage circular polarization (*broken line*) structure in Hα for a dipolar field ($a = 0.0$). The polar field Hα is 40 million gauss. The three pairs of profiles correspond to different inclinations of the magnetic axes on the line of sight ($i = 0°.0, 45°, 90°$).

could be identified as Hα. This is, however, another cool object (Greenstein 1974), and we cannot exclude a weak line.

e) G227–35

A scan by Greenstein (1974) shows a dip at ~4550 Å and another one at ~6500 Å. The latter, if real, could possibly be due to Hα. However, the identification is not sustained by the circular polarization scan published by Angel, Hintzen, and Landstreet (1975).

VI. CONCLUSIONS

The line profiles in Figures 2–7 should serve as a guide in identifying Hα in magnetic white dwarfs. We can give the following rules for finding DA white dwarfs with very strong magnetic fields. If the blue spectrum is featureless or presents weak unidentified features, the star is a good candidate. A red spectrum should then be taken, going, if possible, as red as 8500 Å. For fields from 5×10^7 to 10^8 gauss, Hα should be recognized by its sharp σ^+ features or, if the resolution is insufficient, by the single broad feature at ~7100 Å. The π components should normally be also present, but the σ^- components should be too weak to be observable. For fields less than 5×10^7 gauss, finding Hα will be trivial as it will look like a classical Zeeman triplet. The polarization of the features should be fairly large if Hα is strong but not if it is weak.

We do not see a convincing presence of Hα in any of the polarized white dwarfs (excluding of course G99–47), with perhaps the exception of HD 229. We cannot, however, exclude a weak line in the cooler objects.

This research was supported by the National Research Council of Canada.

REFERENCES

Aller, L. H. 1963, *The Atmospheres of the Sun and Stars* (New York: Ronald Press).
Angel, J. R. P., Carswell, R. F., Strittmatter, P. A., Beaver, E. A., and Harms, R. 1974, *Ap. J.* (*Letters*), **194**, L47.
Angel, J. R. P., Hintzen, P., and Landstreet, J. D. 1975, *Ap. J.* (*Letters*), **196**, L27.
Angel, J. R. P., and Landstreet, J. D. 1970, *Ap. J.* (*Letters*), **160**, L147.
Angel, J. R. P., Landstreet, J. D., and Borra, E. F. 1976, in preparation.
Borra, E. F. 1973, *Ap. J.*, **183**, 587.
Garstang, R. H., and Kemic, S. B. 1974, *Ap. and Space Sci.*, **31**, 103.
Greenstein, J. L. 1974, *Ap. J.* (*Letters*), **194**, L51.
Greenstein, J. L., Schmidt, M., and Searle, L. 1974, *Ap. J.* (*Letters*), **190**, L27.
Kemic, S. B. 1974*a*, *Ap. J.*, **193**, 213.
———. 1974*b*, JILA Reprint, No. 113.
Lamb, F., and Sutherland, P. 1974, in *IAU Symposium 53, Physics of Dense Matter*, ed. C. J. Hansen (Dordrecht: Reidel), p. 265.
Landstreet, J. D. 1970, *Ap. J.*, **159**, 1001.
Landstreet, J. D., and Angel, J. R. P. 1974, *Ap. J.* (*Letters*), **190**, L25.
———. 1975, *Ap. J.*, **196**, 819.
Liebert, J., Angel, J. R. P., and Landstreet, J. D. 1975, *Ap. J.* (*Letters*), **202**, L139.
O'Connell, R. F. 1974, in *IAU Symposium 53, Physics of Dense Matter*, ed. C. J. Hansen (Dordrecht: Reidel), p. 287.
Oke, J. B., and Shipman, H. 1971, in *White Dwarfs*, ed. W. J. Luyten (Dordrecht: Reidel).
Preston, G. W. 1970, *Ap. J.* (*Letters*), **160**, L143.
Trimble, V., and Greenstein, J. L. 1972, *Ap. J.*, **177**, 441.
Wickramasinghe, D. T., and Bessell, M. S. 1976, *Ap. J.* (*Letters*), **303**, L39.

E. F. Borra: Département de Physique, Faculté des Sciences et de Génie, Pavillon Vachon, Université Laval, Québec, P.Q., Canada, G1K 7P4